Pattern Recognition, Vol. 25, No. 1, pp. 45–54, 1992
Printed in Great Britain

0031-3203/92 $5.00 + .00
Pergamon Press plc

AN ADAPTIVE METHOD FOR IMAGE REGISTRATION

JAN FLUSSER
Institute of Information Theory and Automation, Czechoslovak Academy of Sciences,
Pod vodarenskou vezi 4, 182 08 Prague 8, Czechoslovakia

(*Received* 7 *December* 1990; *in final form* 3 *June* 1991; *received for publication* 7 *June* 1991)

Abstract — The paper deals with the registration of images with non-linear local geometric distortions. It describes a new approach to the determination of a mapping function from given coordinates of control points. The processed image is recursively divided into subregions of various size and shape according to the distortion character. Each subregion is then transformed by a simple local transformation. The described method enables the registration with optional accuracy. A practical use of this method is presented and a comparison of its accuracy and computing complexity with previously published methods is given.

Image registration Geometric distortion Mapping function Surface spline Adaptive mapping.

1. INTRODUCTION

The analysis of two or more digital images of the same scene taken from different places or at a different time often requires registration of the images.

Image registration is the process of overlaying two images of the same scene. This process is used in multitemporal analysis of remotely sensed data, in environmental change detection, in medical imaging and in robot vision.

Image registration consists of three main steps:

(1) selection of control points in the reference and sensed images and determination of the correspondence between them;

(2) determination of the type and parameters of the mapping function using known coordinates of control points; and

(3) geometric transformation of the sensed image by means of the mapping function.

In the past, many methods of control point selection have been published. Stockman *et al.*[1] use line intersections as control points and determine the correspondence between them by the means of cluster analysis. Anuta,[2] Barnea and Silverman[3] and Davis and Kenue[4] use window centres as control points and by image correlation establish the correspondence between them. Ton and Jain[5] and Goshtasby *et al.*[6] use centres of gravity of closed boundary regions as control points and by a relaxation process determine corresponding points in the images.

The determination of the concrete mapping function is very important for the accuracy of registration. It has two parts—selection of the appropriate type of function and determination of its parameters from given control point coordinates.

Several authors[6–9] use polynomials of low degrees as mapping functions. Their coefficients are determined by the least-squares technique in such a way that the mapping function minimizes the sum of the squared error at control points. This procedure gives very good results assuming that both images were taken by a perfect camera, that the scene is flat and that the geometric distortion between images has no local factors.

Images of 3D scene, obtained from different viewing angles or from different sensors, have local geometric distortions that depend on the local 3D structure of the scene. Sensor non-linearity and random factors can also contribute to the local distortions.

It is evident that global polynomial mapping cannot achieve accurate registration of images with local distortions. This has been proved by the experiments of Goshtasby.[10,11]

Goshtasby[10–12] proposed several types of local sensitive mapping functions. Piecewise linear[10] and piecewise cubic[12] mapping functions assume triangulation of both images. Vertices of the triangles are used as control points. For each triangle, a corresponding linear or cubic mapping function is then found. The disadvantage of the first method is low accuracy, and the disadvantage of the second method is considerable computing complexity.

The most accurate results of registration of images with local distortions were obtained by using the surface spline mapping functions.[11] As shown below, their direct use has extreme computing complexity and is not suitable for practical applications.

In this paper, a new adaptive method for the determination of the mapping function is presented. This method is able to register images considerably faster than previous methods but with the possibility of reaching comparable accuracy.

In Section 2, image registration as a surface-fitting problem is formulated and surface spline mapping

functions are derived. In Section 3, a new adaptive mapping algorithm is presented and its several modifications are discussed. In Section 4, practical applications of the adaptive mapping algorithm are presented and the proposed image registration technique is compared with the previously published ones.

2. SURFACE SPLINE MAPPING FUNCTION

Let us denote (x, y) and (u, v) coordinates in the sensed and reference image, respectively. Let the geometric distortion between the images be described by unknown functions α, β:

$$u = \alpha(x, y),$$
$$v = \beta(x, y). \tag{1}$$

Let us assume that the positions of n corresponding control points in the images $((x_i, y_i), (u_i, v_i), i = 1, \ldots, n)$ are given and their mutual correspondence is established, e.g.

$$u_i = \alpha(x_i, y_i),$$
$$v_i = \beta(x_i, y_i) \quad i = 1, \ldots, n. \tag{2}$$

We would like to find mapping functions f and g in such a way that the image registration represented by

$$u = f(x, y),$$
$$v = g(x, y), \tag{3}$$

would be as accurate as possible (e.g. the distances $\|f - \alpha\|$, $\|g - \beta\|$ should be small in some functional norm) and that f and g would map corresponding control points exactly on top of each other, e.g.

$$u_i = f(x_i, y_i),$$
$$v_i = g(x_i, y_i) \quad i = 1, \ldots, n. \tag{4}$$

We can formulate this task as a 3D interpolation problem on an arbitrary point set. Given two sets of 3D points

$$S = \{(x_i, y_i, u_i) | i = 1, \ldots, n\}$$
$$Q = \{(x_i, y_i, v_i) | i = 1, \ldots, n\}$$

we would like to find smooth surfaces $f(x, y)$ and $g(x, y)$. The surface $f(x, y)$ has to pass through all points of S and the surface $g(x, y)$ has to pass through all points of Q. We find a minimal solution of the functional of energy

$$J(f) = \int_{R^2}\int \left[\left(\frac{\delta^2 f}{\delta x^2}\right)^2 + 2\left(\frac{\delta^2 f}{\delta x \delta y}\right)^2 + \left(\frac{\delta^2 f}{\delta y^2}\right)^2\right] dx dy \tag{5}$$

on Sobolev's space $W_2^2(R^2)$. Providing that the set of known points includes at least three non-collinear points, the problem has an unambiguous solution[13]

$$u \equiv f(x, y) = a_0 + a_1 x + a_2 y + \sum_{i=1}^{n} F_i r_i^2 \ln r_i^2, \tag{6}$$

where $r_i^2 = (x - x_i)^2 + (y - y_i)^2$. This function f is called surface spline function.

Parameters a_0, a_1, a_2, F_i, $i = 1, \ldots, n$ are determined by substituting of the control point coordinates into Equation (6) and by solving of the system of $(n + 3)$ linear equations

$$f(x_i, y_i) = u_i \quad i = 1, \ldots, n$$
$$\sum_{j=1}^{n} F_j = 0$$
$$\sum_{j=1}^{n} F_j x_j = 0 \tag{7}$$
$$\sum_{j=1}^{n} F_j y_j = 0.$$

The obtained surface $f(x, y)$ represents the first component of the mapping function. The surface $g(x, y)$ representing the second component is determined similarly.

Now it is possible to transform the sensed image pixel by pixel using the functions f and g. In this way the mapping function is sensitive to local geometric distortions between the images and the registration error at the control points is identically zero. But the computing complexity of this step is considerable: having 50 control points and the size of image 512×512 pixels, roughly 2.6×10^7 calculations of logarithmic value would be necessary.

3. ADAPTIVE MAPPING ALGORITHM

The new adaptive mapping (AM) algorithm consists of dividing the sensed image into smaller subregions of simple shapes (squares, triangles, etc.). In each of these subregions, the local approximation of the surface spline functions f, g by more simple mapping functions p, q is performed

$$u = p(x, y),$$
$$v = q(x, y). \tag{8}$$

The size of each subregion is adaptively determined by the algorithm depending on the real character of distortion between the images. In such a way, the approximation error on each subregion is smaller than the parameter δ given in advance by the user.

The main part of the AM algorithm is formed by a recursive procedure TRANS which can be applied on an arbitrary region of the sensed image. In this region, the procedure replaces the spline functions f, g (Equation (6)) by the local mapping functions p, q and calculates the error σ of this approximation. If $\sigma \leq \delta$, the region is transformed by functions p, q. If $\sigma > \delta$, the region is divided into subregions and

the procedure TRANS is repeated on each of them separately. In the first step of the AM algorithm, the procedure TRANS is applied on the whole image.

More formally, the AM algorithm can be described as follows.

AM Algorithm

begin
  read coordinates of control points
  determine the coefficients of functions f, g (Equation (6)) by solving the linear system of Equations (7)
  read δ
  TRANS (image)
end

procedure TRANS (region)
  compute the coefficients of functions p, q
  begin
    let (x_j, y_j), $j = 1, \ldots, m$ are arbitrary points in region
    for $j = 1$ **to** m **do**

$$\sigma_j^2 = (f(x_j, y_j) - p(x_j, y_j))^2 + (g(x_j, y_j) - q(x_j, y_j))^2$$

    endfor
  end

$$\sigma = \frac{1}{m} \sum_{j=1}^{m} \sigma_j$$

begin
  if $\sigma \leq \delta$ **then** transform the region by p, q
    else divide the region into k subregions
      for $i = 1$ **to** k **do**
        TRANS (subregion(i))
  endif
end
end

The accuracy of the image registration by use of the AM algorithm is affected by two kinds of errors. The primary error is caused by inaccuracy with which the functions f and g describe the real distortion between the reference and sensed images. If a sufficient number of control points was selected and if the control points are conveniently distributed over the image, the primary error is negligible.

The secondary error is caused by inaccurate approximation of the functions f, g by the functions p, q. This error can be regulated by reducing the value of the parameter δ. The influence of the parameter δ on the accuracy of image registration and on the time of computing will be demonstrated in Section 4.

The above described AM algorithm has many modifications. These modifications differ from each other by a division of the image into subgroups, by shape of the subregions and by used local mapping functions p, q. In this paper, four versions of the AM algorithm are investigated.

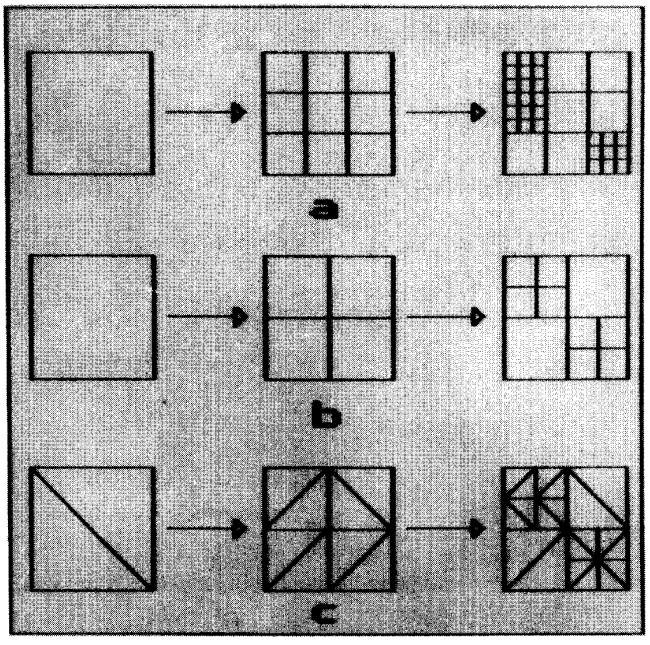

Fig. 1. Possible dividing of the image during the AM algorithm: (a) APM, ABM; (b) ABM2; (c) AAM.

3.1. *Adaptive projective mapping (APM)*

The APM algorithm uses the projective functions

$$u \equiv p(x,y) = (p_0 + p_1x + p_2y)/(1 + c_1x + c_2y),$$
$$v \equiv q(x,y) = (q_0 + q_1x + q_2y)/(1 + c_1x + c_2y), \tag{9}$$

as local mapping functions. Because the functions (9) are unambiguously defined by four points, the algorithm divides the sensed image into square subregions (Fig. 1(a)). The projective transformation preserves straight lines in the transformed image, but does not preserve the continuity of lines at the subregion boundary. The use of projective functions is relatively time consuming. Transformation using more simple local functions is described below.

3.2. *Adaptive bilinear mapping (ABM)*

The ABM algorithm uses the bilinear functions

$$u \equiv p(x,y) = p_0 + p_1x + p_2y + p_3xy,$$
$$v \equiv q(x,y) = q_0 + q_1x + q_2y + q_3xy, \tag{10}$$

as local mapping functions and the division scheme is the same as in the case of the APM. Bilinear transformation preserves the continuity of lines at the boundary of subregions of the same size, but does not preserve straight lines. Compared with the APM algorithm, the computing complexity of the ABM algorithm is lower.

3.3. *Adaptive bilinear mapping 2 (ABM2)*

The ABM2 algorithm uses the same mapping functions as the ABM algorithm, but the division of the image into subregions is different and more levels of recursion are used (see Fig. 1(b)).

3.4. *Adaptive affine mapping (AAM)*

The AAM algorithm uses the affine functions which are very simple for computing

$$u \equiv p(x,y) = p_0 + p_1x + p_2y,$$
$$v \equiv q(x,y) = q_0 + q_1x + q_2y, \tag{11}$$

as local mapping functions. Because the affine functions (11) are unambiguously defined by three noncollinear points, the triangle division scheme is requested (Fig. 1(c)).

4. RESULTS

To measure the performance of the proposed technique for the registration of images with local geometric distortions, the following four experiments were carried out.

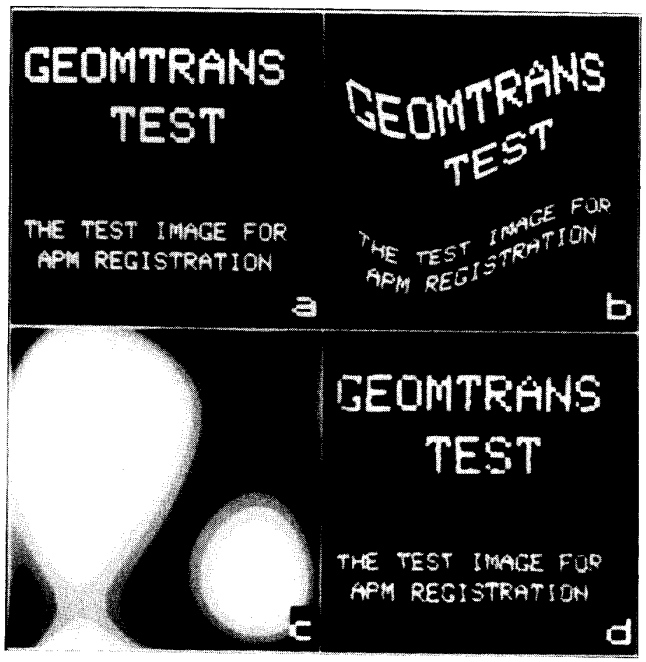

Fig. 2. Experiment on the test image: (a) reference image (256 × 256 pixels); (b) sensed image; (c) visualization of distortion between reference and sensed images; (d) transformation of the sensed image using the surface spline function.

4.1. *Experiment* 1

The first experiment was made on the artificially formed test image. The dependence of accuracy and time of transformation on the parameter δ was investigated in the case of the APM algorithm. The behaviour of the other modifications is very similar. The comparison with the registration results obtained by direct use of the surface splines as the mapping functions is shown.

The test image (Fig. 2(a)) of size 256 × 256 pixels was formed by a graphic editor. The image was deformed by a combination of cubic polynomials and goniometric functions (Fig. 2(b)). These two images are our reference and sensed images, respectively. In Fig. 2(c), the character of distortion between both images is visualized. The white colour corresponds to the greatest space changes.

A set of 50 control points which were used in determination of mapping function coefficients was selected in the reference and sensed images. Also 22 check points were selected which served exclusively for monitoring the accuracy of executed registrations. The intersections of edges of given objects were used as the control points and the check points.

By solving of the system of Equations (7), the coefficients of the surface spline functions f, g were obtained and the sensed image was transformed by means of them. The result of transformation is shown in Fig. 2(d). The visual comparison with the reference image shows the excellent registration quality. The average error at the control points is zero; at the check points it is 0.59 pixels.

Now we use the algorithm APM for the image registration. We vary the value of the parameter δ from 10 to 0.1 and we study the influence of this parameter on the time of processing and on the average registration error.

In Figures 3 and 4 we can observe the influence of

Table 1. The influence of parameter δ on accuracy and time of transformation

δ	σ_1 (pixels)	σ_2 (pixels)	Time (%)
10.0	4.60	5.11	0.8
8.0	3.02	3.08	1.2
6.0	2.14	2.08	1.4
3.0	1.25	1.40	1.6
1.5	0.72	0.94	2.6
1.0	0.59	0.78	4.7
0.5	0.38	0.74	11.7
0.1	0.16	0.68	53.9
Spline	0.00	0.59	100.0

σ_1—average error at control points.
σ_2—average error at check points.

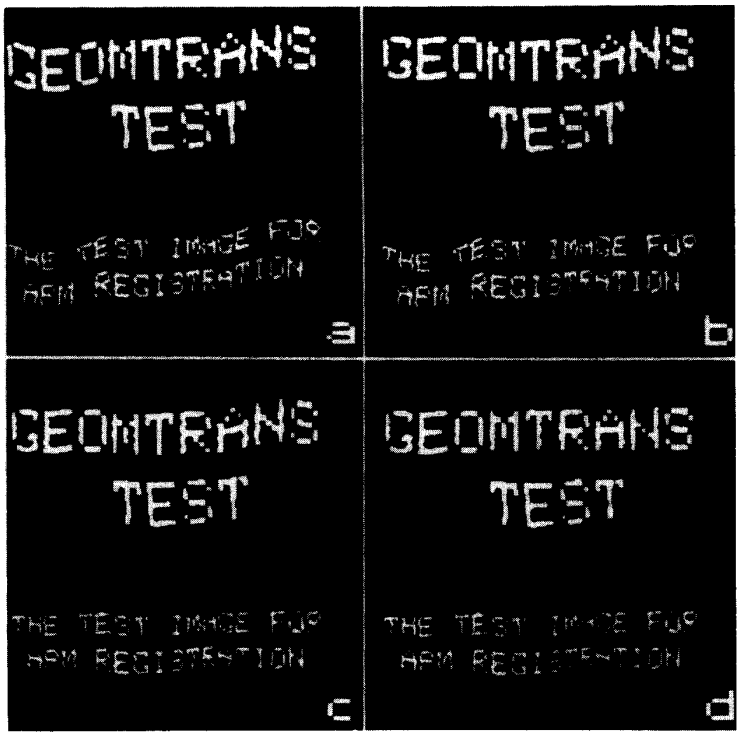

Fig. 3. Transformation of the sensed image using the APM algorithm: (a) $\delta = 10$; (b) $\delta = 8$; (c) $\delta = 6$; (d) $\delta = 3$.

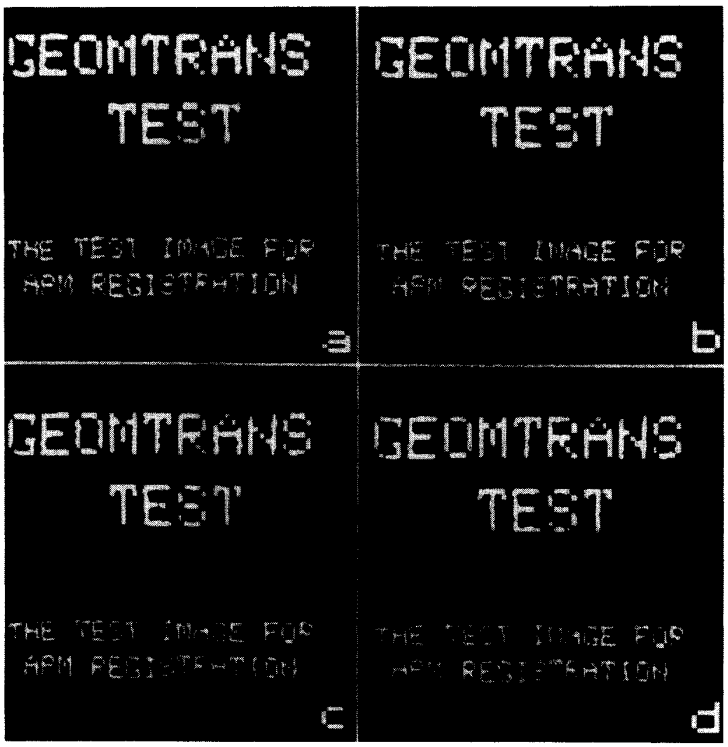

Fig. 4. Transformation of the sensed image using the APM algorithm (continued): (a) $\delta = 1.5$; (b) $\delta = 1.0$; (c) $\delta = 0.5$; (d) $\delta = 0.1$.

reducing parameter δ on the quality of the transformed image. The errors at the control points and at the check points are shown in Table 1. Simultaneously we can watch the time of transformation and we can compare it with the time necessary for the transformation by the surface spline functions. (Note that time of transformation = time of computing of the coefficients + time of geometric transformation of the sensed image.) We compare the time relatively (time for surface spline function = 100%), because the absolute time is considerably affected by the type of the used computer. (In our case, the computer Hewlett Packard 21MX was used and the time for surface spline transformation was 252 min.) All monitored values are shown in Table 1.

4.2. *Experiment* 2

The aim of the second experiment was to compare the algorithms APM, ABM, ABM2 and AAM.

The reference and sensed images from Experiment 1 were used. The sensed image was transformed twice by all modifications of the AM algorithm, values of the parameter $\delta = 6$ and 0.5 were used. The time and the errors of transformations are shown in Table 2. The transformed images are shown in Fig. 5. The divisions of the image into subregions are visualized in Fig. 6.

As is visible from Table 2, there are no significant differences among the APM, ABM, ABM2 and AAM algorithm in the case of $\delta = 6$. In the case of $\delta = 0.5$, the ABM2 algorithm is slightly faster than the others. This is made by the convenient division of the image (see Fig. 6—there are less subregions in Fig. 6(c) than in Figs 6(a), (b) and (d), respectively).

Table 2. Comparison of the APM, ABM, ABM2 and AAM methods (see Experiment 2)

	$\delta = 6$			$\delta = 0.5$		
Method	σ_1	σ_2	Time	σ_1	σ_2	Time
APM	2.14	2.08	2:55	0.38	0.74	22:45
ABM	1.84	1.83	2:35	0.40	0.72	15:20
ABM2	3.66	3.81	1:49	0.33	0.65	12:40
AAM	2.71	2.99	2:08	0.36	0.59	16:05

σ_1—average error at control points.
σ_2—average error at check points.
The σ_i are given in pixels and the time of transformation is given in min:s.

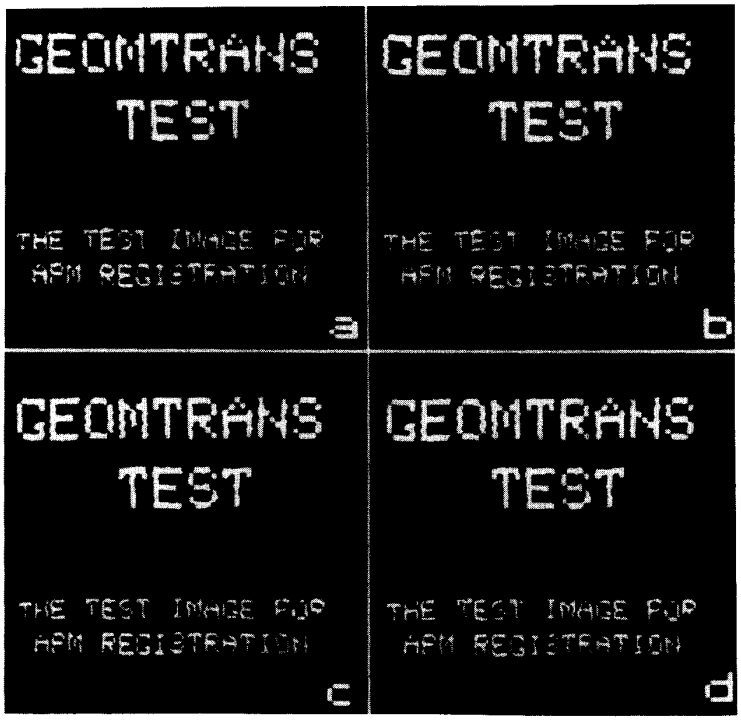

Fig. 5. Transformation of the sensed image using various modifications of the AM algorithm ($\delta = 0.5$): (a) APM; (b) ABM; (c) ABM2; (d) AAM.

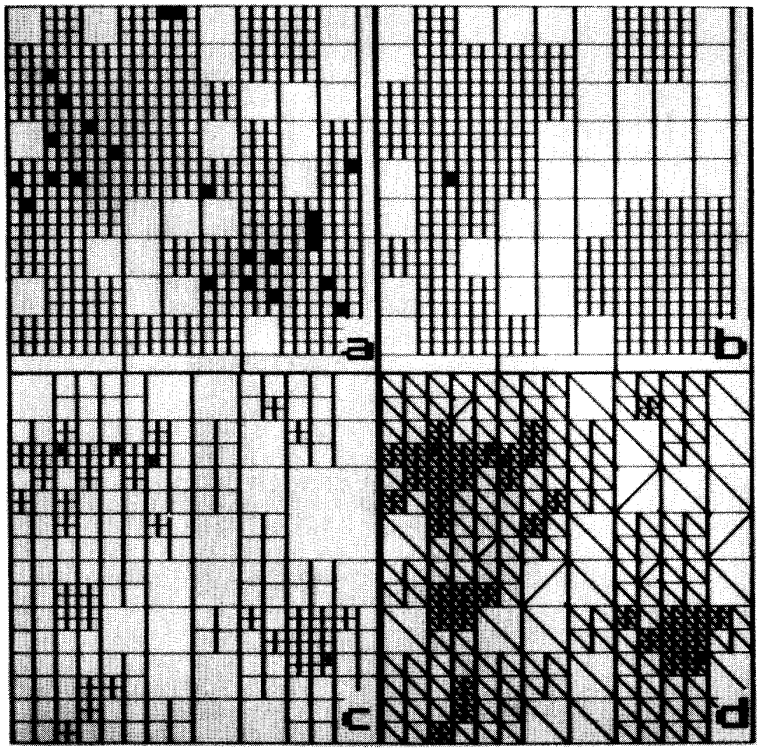

Fig. 6. Dividing of the sensed image into subregions at $\delta = 0.5$ (according to Fig. 5): (a) APM; (b) ABM; (c) ABM2; (d) AAM.

4.3. *Experiment* 3

In the following experiment, the registration of real images is demonstrated.

In Fig. 7(a), the portrait photograph which serves as the reference image is shown. The sensed image was obtained by artificial deformation of the reference image (see Fig. 7(b)). A set of 21 control points was selected in both images. The ABM2 algorithm was used for transformation (value of the parameter $\delta = 2$). The result is shown in Fig. 7(c). The average error at control points was only 0.62 pixels.

4.4. *Experiment* 4

The aim of the fourth experiment was to verify the use of the APM algorithm for the registration of multitemporal aerial images.

Two images of the same scene were taken by a videocamera, each of them at a different time and from a different position of the aircraft (Figs 8(a) and (b)). In both images 17 control points were selected. Their coordinates were determined and their mutual correspondence was established. The first image (Fig. 8(a)) was used as a reference one, the second image (Fig. 8(b)) was transformed by the APM algorithm.

The result of the registration can be seen in Fig. 8(c) (the value of the parameter $\delta = 1$ was used and the average error at the control points was only 0.41 pixels).

A registration of the same images in a classical way was made for comparison—as a mapping function a polynomial of degree two was used and its coefficients were determined by the least-squares technique. The transformed image is shown in Fig. 8(d). The bad quality of this registration (the average error is 5.6 pixels) is caused by the local character of distortion between the reference and sensed images that the polynomial cannot accurately describe.

5. CONCLUSIONS

The paper deals with the registration of two digital images of the same scene with complex local geometric distortions. This requirement appears very often in the processing of low altitude multispectral or multitemporal aerial images of the Earth's surface.

Attention was paid to the discovery of sufficiently accurate mapping functions which would enable faster image registration than the mapping functions used until now.

In Section 3, the adaptive mapping algorithm (AM) was presented. It represents a new approach

Fig. 7. Exp :al image: (a) reference image (256 × 256 pixels); (b) sensed image; (c) formation of the sensed image using the ABM2 algorithm, $\delta = 2$.

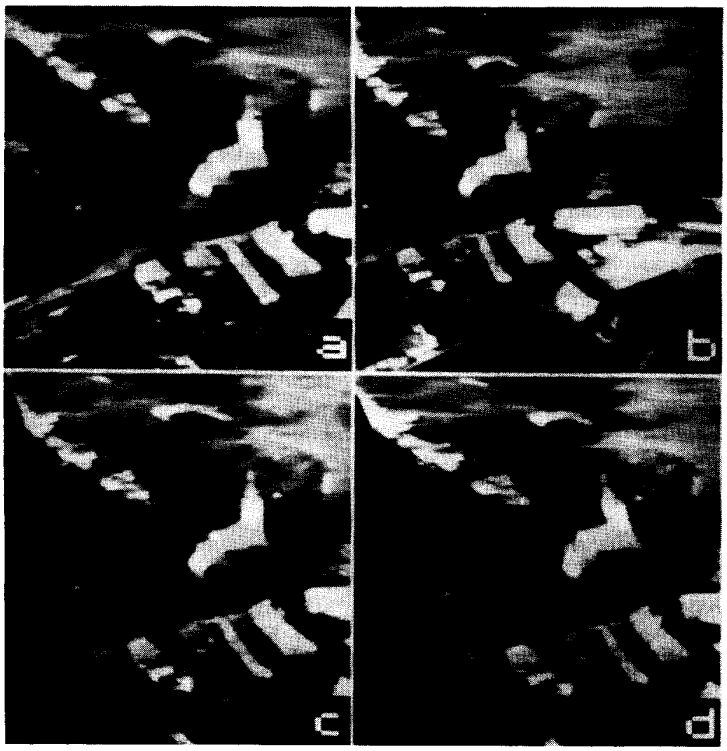

Fig. 8. Aerial images: (a) reference image; (b) sensed image; (c) image registration using the APM algorithm, $\delta = 1$; (d) image registration using the polynomial mapping.

to the determination of the mapping function. This approach consists of adaptive dividing of the image into subregions and the local transformation of these subregions by simple mapping functions. Four modifications of the AM algorithms were described and their properties were discussed.

In Section 4, the use of this method for the registration of images with local distortions was verified by experiments and the results were compared with the result of registration by means of the surface spline functions. It was shown that the AM technique can reach comparable accuracy at a considerably reduced time of computing.

The parameter δ defines the requested accuracy of transformation in the AM algorithm. The possibility of optional reduction of the time of processing by the reduction of the requested accuracy is a great advantage of the AM algorithm.

The experimental comparison between the APM, ABM, ABM2 and AAM algorithms shows that the efficiency of these methods (e.g. computing complexity and accuracy) is roughly equal. The choice of the most suitable algorithm depends on actual character of given images and on the user's requests.

The registration of multitemporal aerial images was carried out by means of the APM algorithm and the subpixel registration accuracy was reached.

The described technique can be successfully used for the registration of any images regardless of the distortion character and independent of the number, position and mode of selection of control points. But its most efficient application is for images with complex local distortions.

6. SUMMARY

A new approach for the determination of the mapping function for the registration of digital images with complex geometric distortions is presented.

Given the coordinates of corresponding control points in two images of the same scene, first the coefficients of surface spline mapping function are calculated. Then the image is adaptively divided into subregions of various size according to the character of distortion. The surface spline function is approximated in each of these subregions by simple local mapping functions. Then each subregion is transformed separately.

Four modifications of the adaptive mapping algorithm were investigated. To measure their performance for image registration, many experiments on the test and real images were carried out. Results of the experiments are presented.

It was proved that the adaptive mapping technique can reach comparably accurate results as the previously published methods.

The relation between the time of processing and the registration accuracy can be regulated by the parameter δ given by the user. This fact is one of the main advantages of the AM algorithm.

The described technique can be successfully used for the registration of any images regardless of the distortion character and independent of the number, position and mode of selection of control points. But its most efficient application is for images with complex local distortions.

REFERENCES

1. G. C. Stockman, S. Kopstein and S. Benett, Matching images to models for registration and object detection via clustering, *IEEE Trans. Pattern Anal. Mach. Intell.* **4**, 229–241 (1982).
2. P. E. Anuta, Digital registration of multispectral video imagery, *Soc. Photo-Optical Instrum. Engrs J.* **7**, 168–175 (1969).
3. D. I. Barnea and H. F. Silverman, A class of algorithms for fast digital image registration, *IEEE Trans. Comput.* **21**, 179–186 (1972).
4. W. A. Davis and S. K. Kenue, Automatic selection of control points for the registration of digital images. In *Proc. 4th Int. jt Conf. Pattern Recognition*, pp. 936–938 (1978).
5. J. Ton and A. K. Jain, Registering Landsat images by point matching, *IEEE Trans. Geosci. Remote Sensing* **27**, 642–651 (1989).
6. A. Goshtasby, G. C. Stockman and C. V. Page, A region-based approach to digital image registration with subpixel accuracy, *IEEE Trans. Geosci. Remote Sensing* **24**, 390–399 (1986).
7. D. Steiner and M. E. Kirby, Geometrical referencing of Landsat images by affine transformation and overlaying of map data, *Photogrammetria* **33**, 41–75 (1977).
8. P. Van Wie and M. Stein, A Landsat digital image rectification system, *IEEE Trans. Geosci. Electron.* **15**, 130–137 (1977).
9. J. Flusser, Geometrical transformations of remotely sensed data. In *Proc. Digital Image Process. '88*, Prague, pp. 92–96 (1988).
10. A. Goshtasby, Piecewise linear mapping functions for image registration, *Pattern Recognition* **19**, 459–466 (1986).
11. A. Goshtasby, Registration of images with geometric distortions, *IEEE Trans. Geosci. Remote Sensing* **26**, 60–64 (1988).
12. A. Goshtasby, Piecewise cubic mapping functions for image registration, *Pattern Recognition* **20**, 525–533 (1987).
13. W. E. L. Grimson, A computational theory of visual surface interpolation, *Phil. Trans. R. Soc. Lond. B* **298**, 395–427 (1982).

About the Author — JAN FLUSSER was born in Prague, Czechoslovakia, on 30 April 1962. He received an M.Sc. degree in Mathematical Engineering from the Czech Technical University of Prague, Czechoslovakia, in 1985 and Ph.D. degree in Computer Science from the Czechoslovak Academy of Sciences, Prague, in 1990.

He is employed by the Institute of Information Theory and Automation, Czechoslovak Academy of Sciences. His research interests include digital image processing and remote sensing.